

# Scalable and Continuous Water Deionization by Shock Electrodialysis

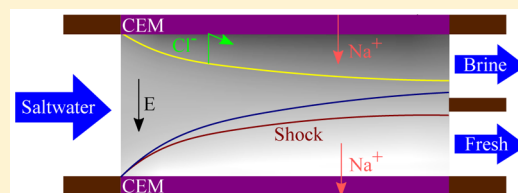
Sven Schlumpberger,<sup>†</sup> Nancy B. Lu,<sup>†</sup> Matthew E. Suss,<sup>†,§</sup> and Martin Z. Bazant<sup>\*,†,‡</sup>

<sup>†</sup>Department of Chemical Engineering, Massachusetts Institute of Technology, Cambridge, Massachusetts 02139, United States

<sup>‡</sup>Department of Mathematics, Massachusetts Institute of Technology, Cambridge, Massachusetts 02139, United States

**S** Supporting Information

**ABSTRACT:** Rising global demand for potable water is driving innovation in water treatment methods. Shock electro-dialysis is a recently proposed technique that exploits deionization shock waves in porous media to purify water. In this letter, we present the first continuous and scalable shock electro-dialysis system and demonstrate the separation of sodium, chloride, and other ions from a feed stream. Our prototype continuously removes over 99% (and up to 99.99%) of salt from diverse electrolytes over a range of concentrations (1, 10, and 100 mM). The desalination data collapse with dimensionless current, scaled to charge advection in the feed stream. Enhanced water recovery with increasing current (up to 79%) is a fortuitous discovery, which we attribute to electro-osmotic pumping. These results suggest the feasibility of using shock electro-dialysis for practical water purification applications.



## INTRODUCTION

Access to potable water is a critical global challenge. It is estimated that more than one billion people currently do not have reliable access to clean and safe water.<sup>1</sup> Unfortunately, the purification of nonpotable water is infrastructure-intensive and expensive, as many countries currently supplement their water supply with seawater desalination by large-scale reverse osmosis (RO), or in some cases electro-dialysis (ED).<sup>2,3</sup> Moreover, widespread interest in purifying wastewater has intensified with the ascent of hydraulic fracturing for shale gas extraction, which is difficult to treat because of the presence of large amounts of dissolved salts.<sup>4–6</sup> For these and other applications, extensive research is underway to develop improved water treatment methods, and the unique capabilities of electrochemical systems have attracted renewed attention.<sup>7–10</sup>

One of the new electrochemical approaches to water purification is shock electro-dialysis (SED),<sup>11–13</sup> which is based on the emerging science of deionization shocks in porous media.<sup>14–23</sup> The SED process involves flowing feedwater through a weakly charged porous slab with micrometer-sized pores that is placed between two ion-selective elements, such as ion-exchange membranes or electrodes. When current is passed through the device, zones of ion depletion and enrichment are formed to maintain electro-neutrality near the ion-selective surfaces. In the classical picture, a diffusion-limited current is reached whenever the salt concentration approaches zero, but it is well established that overlimiting currents are possible in bulk electrolytes because of electrokinetic or electrochemical phenomena,<sup>10</sup> such as the Rubinstein–Zaltzman electro-osmotic instabilities<sup>24–27</sup> or current-induced membrane discharge.<sup>28</sup> Recently, it has been shown that two new mechanisms,<sup>18</sup> surface conduction (by electromigration)<sup>19,20</sup> and surface convection (by electro-osmosis),<sup>21,29,30</sup> are responsible for overlimiting current when the electrolyte is confined in a microchannel<sup>18,23,31</sup> or porous

medium,<sup>12,32</sup> whose surface charge is the opposite of that of the active ionic species. The transient response to an applied overlimiting current (discovered first in 2009<sup>15,16</sup>) is the propagation of a deionization shock wave through the microchannel or porous medium with a sharp boundary between concentrated and depleted zones.<sup>14,17,19,20,33</sup> Stationary deionization shocks were first observed at nanochannel junctions<sup>34</sup> and can cause localized seawater desalination within a microchannel.<sup>22</sup> For SED in porous media,<sup>11,12</sup> the flow of water can also be separated into brine and depleted streams by a physical splitter that is placed within the location of the shock in a pressure-driven cross-flow. The basic physics of SED was recently demonstrated in a noncontinuous copper electro-deposition cell that was able to reduce the concentration of copper sulfate by five orders of magnitude in two passes<sup>12</sup> and perform other separations and disinfection<sup>13</sup> through a silica glass frit.

In this letter, we report the first continuous and scalable SED system for arbitrary feed streams. We characterized its voltage response using IV curves and tested its capability to desalinate NaCl solutions at concentrations of 1, 10, and 100 mM, as well as KCl, KNO<sub>3</sub>, and Na<sub>2</sub>SO<sub>4</sub> solutions at 10 mM. We also made the fortuitous discovery that electro-osmotic (EO) pumping leads to greatly enhanced water recoveries, a feature not captured in existing theoretical SED models.<sup>12,14,15,17–19</sup>

## MATERIALS AND METHODS

Following previously introduced concepts,<sup>11,12,19</sup> the prototype was designed to be continuous and scalable with a novel cross-flow architecture (Figure 1a) that employs two identical ion-

Received: November 3, 2015

Accepted: November 3, 2015

Published: November 3, 2015

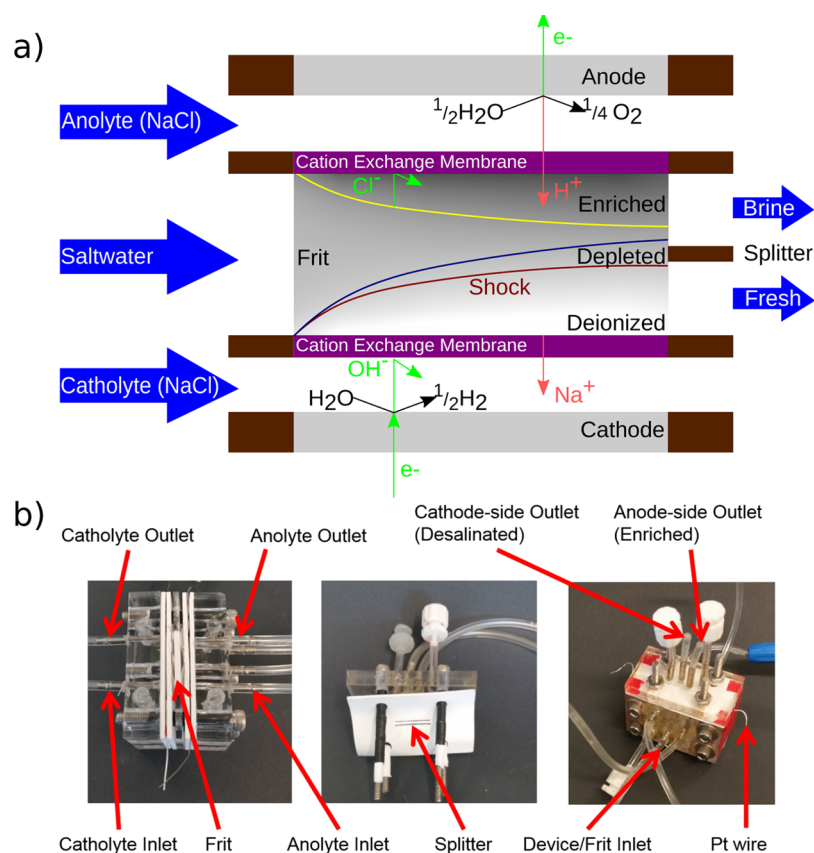


**Figure 1.** (a) Diagram of the SED prototype, showing its operating principles. In the presence of chloride ions, oxidation of chloride ions to hypochlorite ions or chlorine gas may take place in addition to oxygen evolution at the anode. (b) Photographs of the SED prototype, both assembled (right) and unassembled (left and center) to show the frit placement and splitter design.

exchange membranes and a porous frit, which acts as a “leaky membrane” of the same polarity (i.e. a frit with negative surface charge is used with cation-exchange membranes). When an overlimiting current is applied to the system, a deionization shock (sharp concentration gradient) propagates away from the cathode-side membrane and bends in the imposed cross-flow. The deionized solution in its wake is extracted by splitting the flow into two streams at sufficiently high currents (or low flow rates) for the shock to span the freshwater outlet. This structure could be repeated by making a stack of alternating glass frits and membranes, thereby easily scaling the device. Some pictures of the device are shown in Figure 1b.

The main body of the prototype was made from extruded acrylic sheets (W. W. Grainger) and GORE gasket sheets. These materials were cut using a laser cutter to give overall device dimensions of 2 in.  $\times$  2 in.  $\times$  1.5 in. The electrodes were made of platinum mesh connected to platinum wires (Alfa Aesar). The porous material was a silica glass frit (Adams & Chittenden Scientific Glass, ultrafine, pore size of 0.9–1.4  $\mu\text{m}$ , BET internal area ( $a_m$ ) of 1.75  $\text{m}^2/\text{g}$ , mass density ( $\rho_m$ ) of 1.02  $\text{g}/\text{cm}^3$ , porosity ( $\epsilon_p$ ) of 0.31, and dimensions of 20 mm  $\times$  10 mm  $\times$  2.7 mm), and the membranes were Nafion (Ion Power, N115, thickness of  $\sim 127 \mu\text{m}$ ).

Before assembly, the membranes were treated chemically to remove any impurities and to activate them. The frit was glued into its acrylic frame using Devcon 2 Ton Epoxy (McMaster-Carr) before assembly. The gasketing material was used to seal the device and house the electrode channels (each  $\sim 0.8$  mm thick during operation) that had been cut into the gaskets. The electrode channels were open and pressurized during operation

using downstream pressure tubing to hold the membranes flat against the frit. The splitter was also made from Teflon gasketing material that was compressed against the end of the frit using the outlet port plate (see the Supporting Information for more details).

During device operation, flow rates through three syringes were controlled by syringe pumps (Harvard Apparatus). The electrode channels were supplied with an electrolyte solution of the same concentration and composition as the feed to the frit. The flow rates were verified manually at the device outlets before experiments. Current was then applied using a Keithley Instruments Model 2450 SourceMeter. During desalination tests, the system was allowed to reach steady state before samples were taken from the outlets for impedance measurements using a Gamry Reference 3000 Potentiostat to determine their conductivities.

## RESULTS AND DISCUSSION

The current–voltage relation of the device was obtained by slow linear sweeps in current, because traditional voltage sweeps (cyclic voltammetry) were found to be less stable in the overlimiting regime. Typical polarization curves at a sweep rate of 25  $\text{nA}/\text{s}$  ( $125 \mu\text{A m}^{-2} \text{s}^{-1}$ ) for 10 mM NaCl are shown in Figure 2. Although the current was sustained by water splitting, the onset voltage for significant current was consistently close to 1 V, which is less than the standard potential for water electrolysis (1.229 V), either because of the very low partial pressures of oxygen and hydrogen gas, since no gases were fed to the electrode channels, or because of other reactions, such as

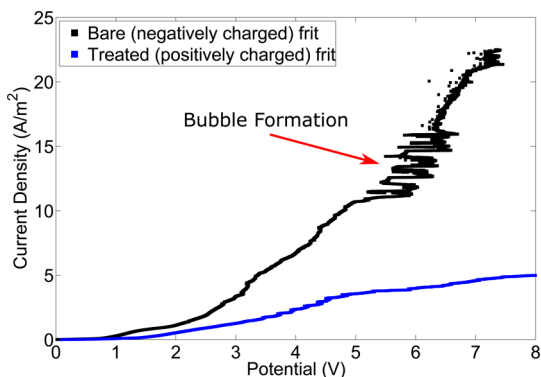


**Figure 2.** Typical current–voltage relations for the SED prototype measured at a sweep rate of 25 nA/s ( $125 \mu\text{A m}^{-2} \text{s}^{-1}$ ) for 10 mM NaCl ( $j_{\text{lim}} \approx 0.33 \text{ A/m}^2$  without convection) with the bare, negatively charged silica glass frit used for desalination (below), as well as a frit whose surfaces are coated with positively charged polymers to show the role of negative surface charge in sustaining an overlimiting current.<sup>12,32</sup> The overlimiting conductance<sup>18</sup> is consistent with electro-osmotic surface convection,<sup>12</sup> and unstable voltage associated with water splitting is observed above  $11 \text{ A/m}^2$  ( $>30j_{\text{lim}}$ ).

the oxidation of chloride ions to hypochlorite ions, occurring. The role of surface transport in overlimiting current was demonstrated by comparing polarization curves for a bare, negatively charged frit used in the desalination experiments (black line in Figure 2) and for a positively charged frit (blue line), whose surfaces had been treated by layer-by-layer

deposition of a charged polymer,<sup>12,32</sup> polydiallyldimethylammonium chloride (pDADMAC). Importantly, the two curves in Figure 2 show significant differences above the same current density where strong desalination is observed in the bare frit (see below), which is well above the theoretical diffusion-limited current density ( $j_{\text{lim}} = 4zeD_{\text{eff}}c_0/L \approx 0.33 \text{ A/m}^2$  for 10 mM NaCl, where  $D_{\text{eff}} = 2.30 \times 10^{-10} \text{ m}^2/\text{s}$  and  $L = 2.7 \text{ mm}$ ) because of convection.<sup>12</sup> After this divergence, for the bare frit, there is a nearly linear increase in current density, as predicted theoretically<sup>18,19</sup> and observed experimentally in previous experiments on overlimiting current in negatively charged porous media<sup>12,32</sup> and microfluidic devices.<sup>23</sup> The overlimiting conductivity (slope  $\times$  thickness of frit) of  $9.79 \times 10^{-3} \text{ S/m}$  is quantitatively consistent with previous experiments with the same porous silica glass frits and Nafion membranes that attributed this phenomenon to electro-osmotic surface convection.<sup>12</sup> At still higher voltages, a nonlinear increase in current density is observed, likely associated with concentration polarization and water splitting in the electrode channels, as in traditional electro dialysis systems.<sup>7,8,10</sup> Bubble formation is observed in the effluent of the electrode streams above  $11 \text{ A/m}^2$  ( $>30j_{\text{lim}}$ ), and the voltage becomes unstable and unreliable.

As noted above, it seems better to operate shock electrochemical systems by controlling the current, rather than the voltage. Recent experiments<sup>12</sup> and simulations<sup>35</sup> have shown that voltage sweeps tend to overshoot and oscillate around the limiting current plateau. In steady state, galvanostatic operation also helps to ensure the formation of a stable deionization

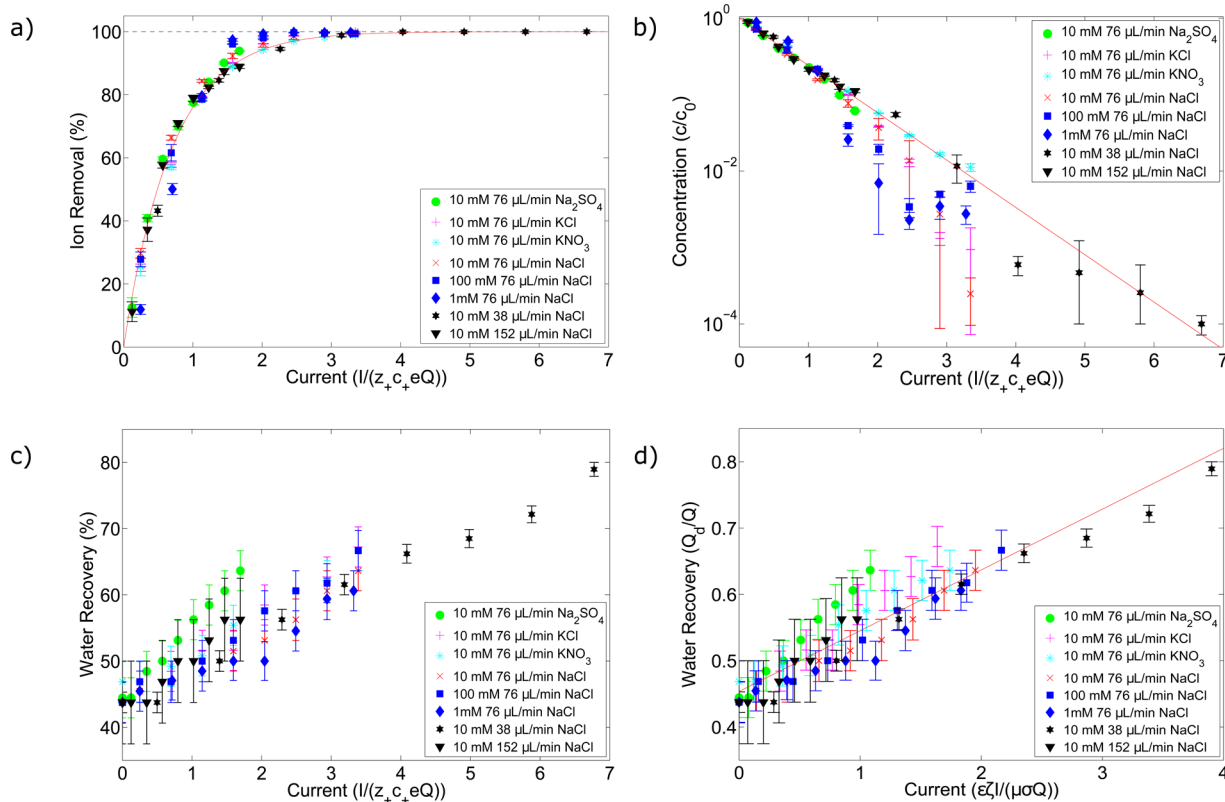


**Figure 3.** Desalination performance of the SED prototype. (a) Collapse of data of the percentage of ion removal,  $1 - \tilde{c}$ , where  $\tilde{c} = c/c_0$  is the ratio of fresh to feed salt concentrations, versus dimensionless current,  $\tilde{I} = I/(z_+ c_+ eQ)$ , scaled to the rate of positive charge advection into the device. (b) This semilog plot of  $\tilde{c}$  vs  $\tilde{I}$  shows excellent data collapse around the red line,  $\log \tilde{c} = -0.619\tilde{I}$ , especially below 95% salt removal. (c) Data for water recovery ( $R_w$ ) vs dimensionless current  $\tilde{I}$ . As shown in panel (d), data collapse is quite good by scaling an estimate of the transverse electro-osmotic flow to the applied flow rate,  $\hat{I} = Q_{\text{EO}}/Q = e\zeta I/(\mu\sigma Q)$ . The red line,  $R_w = 0.454 + 0.092\hat{I}$ , gives a reasonable fit of all the data ( $\chi_{\text{reduced}}^2 = 1.22$ ).

shock by maintaining overlimiting current.<sup>15–17,19,20,23,33</sup> In contrast, potentiostatic operation leads to variable shock speeds in the overlimiting regime,<sup>19,36</sup> and unstable currents at high voltage (from bubble formation and electro-osmotic instabilities in the electrode channels) could disrupt the shock structure required for stable desalination.

Desalination tests were conducted over a wide range of currents, flow rates, and concentrations with several different electrolytes. Figure 3a shows a remarkable collapse of all the data on a single dimensionless curve by plotting the percentage of salt removed  $1 - \tilde{c}$ , where  $\tilde{c} = c/c_0$  is the ratio of fresh to feed salt concentration, versus the applied current scaled to the rate of positive charge advection into the device,  $\tilde{I} = I/z_+c_+eQ$ , where  $Q$  is the inlet flow rate,  $z_+$  is the charge number of the cation,  $e$  is the elementary charge, and  $c_+$  is the inlet concentration of the cation. The master curve is approximately exponential,  $\log \tilde{c} \approx -\gamma\tilde{I}$ ,  $\gamma = 0.619$ , as shown by the semilog plot in Figure 3b. The collapse of data with the dimensionless current further supports the benefits of galvanostatic operation noted above.

In dimensionless variables, the desalination performance of SED is thus mainly controlled by the properties of the porous medium (macroscopic dimensions, surface charge, and microstructure) and does not explicitly depend on the ion type (subject to minor differences in ionic mobilities), salt concentration, current, or flow rate. Simple models of SED predict similar data collapse and improved desalination with an increase in the dimensionless ratio  $\tilde{\rho}_s = q_s a_m \rho_m / 2 \varepsilon_p z_+ e c_+$  of the surface charge ( $q_s$ ) to the feed total ionic charge per macroscopic volume.<sup>19</sup> This trend is consistent with the poor performance of a frit with larger pores and about five-fold smaller  $\tilde{\rho}_s$  (Figure S6 of the Supporting Information), although more experiments are needed to ultimately confirm the predicted scaling.

Counterintuitively, the placement of the splitter is not the sole factor that determines the water recovery (defined as the ratio of flow of desalinated water ( $Q_d$ ) to total flow of water ( $Q$ ) into the frit), in contrast to existing theoretical SED models.<sup>12,14,15,17–19</sup> Because our splitter was placed midway along the frit's downstream edge, the recovery was expected to be approximately 50%, with only small variations due to random pore structure or uncertainty in the splitter placement (because it is made of nonrigid gasketing material). However, as the data in Figure 3c show, the water recovery actually increased from ~45% to 79% with an increase in current and a decrease in flow rate. We hypothesize that this observation can be explained by an increasingly significant contribution of electro-osmotic pumping to the total flow (i.e., the larger the ratio of electro-osmotic flow to applied flow, the higher the water recovery). Porous glass frits, like those we have used in our SED device, have been used as electro-osmotic pumps,<sup>37</sup> and it is known that water pumping is toward the cathode at near-neutral pH.<sup>37,38</sup> In our device with impermeable membranes, however, existing models predict that any transverse electro-osmotic pumping would be opposed by pressure-driven back flow, yielding no change in water recovery.

The resolution of this paradox may come from electro-osmotic surface convection behind the shock,<sup>18,21</sup> which could dissipate the pressure in vortices and redirect the net electro-osmotic flow into the fresh outlet. Such convection has already been implicated as the dominant mechanism for overlimiting conductance in our glass frits<sup>12</sup> and in microchannels with similar vortex sizes.<sup>23</sup> Indeed, the classical model of electro-osmotic pumping without any back pressure<sup>38</sup> predicts

velocities at high currents comparable to the applied velocity. To test this hypothesis, we replot the water recovery ( $R_w$ ) data in Figure 3d versus the ratio of the electro-osmotic pumping rate to the applied flow rate,  $\hat{I} = Q_{EO}/Q$ , where  $Q_{EO} = \varepsilon \zeta I / (\mu \sigma)$  is an estimate of the electro-osmotic flow,  $\varepsilon$  the permittivity,  $\zeta$  the  $\zeta$  potential (set to 100 mV<sup>37</sup>),  $\mu$  the viscosity, and  $\sigma$  the conductivity.<sup>39</sup> This leads to a reasonable collapse of the data on a straight line,  $R_w = \alpha + \beta \hat{I}$ ,  $\alpha = 0.454$ , and  $\beta = 0.092$ , consistent with a simple derivation in the Supporting Information. Statistical analysis gives a reduced  $\chi^2$  value of 1.22, indicating a good fit of the data. The small dimensionless slope (0.092) suggests that electro-osmotic flow is significantly retarded by back pressure or surface charge regulation<sup>12</sup> in the depleted region. Overall, the results strongly suggest that electro-osmotic pumping leads to increased water recovery, which could be exploited in future system designs.

All desalination methods exhibit a trade-off between salt removal, water recovery, and energy efficiency. Plots of total (electrical and hydraulic pumping) energy consumption are shown in Figure S4 of the Supporting Information for all the conditions in Figure 3. In this first SED prototype, the impressive salt removal and water recovery come with significant energy costs, in the range of  $10^{-2}$  to  $10^3$  kWh/m<sup>3</sup> (hydraulic pumping contributes ~0.004 kWh/m<sup>3</sup>). The energy efficiency (ratio of the thermodynamic limit set by osmotic pressure<sup>40</sup> to the actual total energy consumption) varied between 0.67% to 0.073%. The current efficiency peaks at 57.7% at the onset of strong deionization and decays with increasing current toward an apparent lower limit of ~10% (see Figure S5). This novel behavior, compared to current efficiencies of >80% in electrodialysis,<sup>41</sup> suggests that the surface current in the deionized region has a larger transference number for protons than for other cations.

In future SED systems, the energy efficiency may be significantly improved by using a stack of frits and membranes (to reduce the fraction of the total voltage lost to electrolysis) and by varying properties of the porous medium, such as surface charge, proton affinity, matrix microporosity (to enhance salt removal and shock formation), and anisotropic macroporosity (to lower hydraulic resistance in the flow direction). As in traditional desalination plants, the overall energy efficiency could also be improved by harvesting lost heat or reusing the brine and electrode streams in related processes.

In summary, we have shown for the first time that a salt concentration shock wave can be stable and propagate despite continuous cross-flow through a random porous medium, as predicted theoretically for thin shocks in the absence of cross-flow.<sup>17</sup> Thereby, we have demonstrated that SED can be harnessed to continuously and scalably remove  $\geq 99\%$  of ions from electrolyte solutions with water recovery up to 79%, biased by a new mechanism of electro-osmotic pumping. Furthermore, this system can be scaled analogously to electrodialysis systems by repeating our unit cell between two electrodes. In the future, the design of the prototype will be altered to give more precise control of the water recovery by electro-osmotic flow and to improve energy efficiency, guided by the scaling laws revealed in Figure 3. In addition, we will investigate the recycling of the anolyte and catholyte solutions, keeping in mind that the pH of these solutions, when unbuffered, can deviate significantly during operation. Possible applications include wastewater recycling, ultrapure water production, treatment of produced water from hydraulic fracturing, and water disinfection.<sup>13</sup> The enormous gradients

in salt concentration and electric field that arise in SED also provide new opportunities for chemical or biological separations.<sup>13</sup>

## ■ ASSOCIATED CONTENT

### 📄 Supporting Information

The Supporting Information is available free of charge on the ACS Publications website at DOI: [10.1021/acs.estlett.5b00303](https://doi.org/10.1021/acs.estlett.5b00303).

A derivation of the scaling of water recovery with electro-osmotic pumping, more details about the materials and methods, and further plots of desalination performance, energy consumption, and current efficiency (PDF)

## ■ AUTHOR INFORMATION

### Corresponding Author

\*E-mail: [bazant@mit.edu](mailto:bazant@mit.edu). Phone: (617) 324-2036.

### Present Address

<sup>§</sup>M.E.S.: Faculty of Mechanical Engineering, Technion Israel Institute of Technology, Technion City, Haifa 3200003, Israel.

### Notes

The authors declare no competing financial interest.

## ■ ACKNOWLEDGMENTS

This research was supported by Weatherford International, the MIT Energy Initiative, the SUTD-MIT Fellowship Program, and the USA-Israel Binational Science Foundation (Grant 2010199).

## ■ REFERENCES

- (1) Gleick, P. H. The human right to water. *Water Policy* **1998**, *1*, 487–503.
- (2) Shannon, M. A.; Bohn, P. W.; Elimelech, M.; Georgiadis, J. G.; Mariñas, B. J.; Mayes, A. M. Science and technology for water purification in the coming decades. *Nature* **2008**, *452*, 301–310.
- (3) Chao, Y.-M.; Liang, T. M. A feasibility study of industrial wastewater recovery using electrodialysis reversal. *Desalination* **2008**, *221*, 433–439.
- (4) Volesky, B.; Holan, Z. R. Biosorption of heavy metals. *Biotechnol. Prog.* **1995**, *11*, 235–50.
- (5) Wan Ngah, W. S.; Hanafiah, M. A. K. M. Removal of heavy metal ions from wastewater by chemically modified plant wastes as adsorbents: a review. *Bioresour. Technol.* **2008**, *99*, 3935–3948.
- (6) Yavuz, C. T.; Mayo, J.; Yu, W. W.; Prakash, A.; Falkner, J. C.; Yean, S.; Cong, L.; Shipley, H. J.; Kan, A.; Tomson, M.; Natelson, D.; Colvin, V. L. Low-field magnetic separation of monodisperse Fe<sub>3</sub>O<sub>4</sub> nanocrystals. *Science* **2006**, *314*, 964–967.
- (7) Probst, R. *Physicochemical Hydrodynamics: An Introduction*; John Wiley & Sons: New York, 1994.
- (8) Nikonenko, V. V.; Pismenskaya, N. D.; Belova, E. I.; Sizat, P.; Huguet, P.; Pourcelly, G.; Larchet, C. Intensive current transfer in membrane systems: Modelling, mechanisms and application in electrodialysis. *Adv. Colloid Interface Sci.* **2010**, *160*, 101–123.
- (9) Porada, S.; Zhao, R.; van der Wal, A.; Presser, V.; Biesheuvel, P. M. Review on the science and technology of water desalination by capacitive deionization. *Prog. Mater. Sci.* **2013**, *58*, 1388–1442.
- (10) Nikonenko, V. V.; Kovalenko, A. V.; Urtenov, M. K.; Pismenskaya, N. D.; Han, J.; Sizat, P.; Pourcelly, G. Desalination at overlimiting currents: State-of-the-art and perspectives. *Desalination* **2014**, *342*, 85–106.
- (11) Bazant, M. Z.; Dydek, E. V.; Deng, D. S.; Mani, A. Method and apparatus for desalination and purification. U.S. Patent 8,801,910, 2014.
- (12) Deng, D.; Dydek, E. V.; Han, J.-H.; Schlumpberger, S.; Mani, A.; Zaltzman, B.; Bazant, M. Z. Overlimiting Current and Shock Electrodialysis in Porous Media. *Langmuir* **2013**, *29*, 16167–16177.
- (13) Deng, D.; Aouad, W.; Braff, W. A.; Schlumpberger, S.; Suss, M. E.; Bazant, M. Z. Water purification by shock electrodialysis: Deionization, filtration, separation, and disinfection. *Desalination* **2015**, *357*, 77–83.
- (14) Zangle, T. A.; Mani, A.; Santiago, J. G. Theory and experiments of concentration polarization and ion focusing at microchannel and nanochannel interfaces. *Chem. Soc. Rev.* **2010**, *39*, 1014–1035.
- (15) Mani, A.; Zangle, T. A.; Santiago, J. G. On the Propagation of Concentration Polarization from Microchannel-Nanochannel Interfaces: Analytical Model and Characteristic Analysis. *Langmuir* **2009**, *25*, 3898–3908.
- (16) Zangle, T. A.; Mani, A.; Santiago, J. G. On the Propagation of Concentration Polarization from Microchannel-Nanochannel Interfaces: Numerical and Experimental Study. *Langmuir* **2009**, *25*, 3909–3916.
- (17) Mani, A.; Bazant, M. Z. Deionization shocks in microstructures. *Phys. Rev. E* **2011**, *84*, 061504.
- (18) Dydek, E. V.; Zaltzman, B.; Rubinstein, I.; Deng, D. S.; Mani, A.; Bazant, M. Z. Overlimiting Current in a Microchannel. *Phys. Rev. Lett.* **2011**, *107*, 118301.
- (19) Dydek, E. V.; Bazant, M. Z. Nonlinear dynamics of ion concentration polarization in porous media: The leaky membrane model. *AIChE J.* **2013**, *59*, 3539–3555.
- (20) Yaroshchuk, A. Over-limiting currents and deionization “shocks” in current-induced polarization: Local-equilibrium analysis. *Adv. Colloid Interface Sci.* **2012**, *183–184*, 68–81.
- (21) Rubinstein, I.; Zaltzman, B. Convective diffusive mixing in concentration polarization: from Taylor dispersion to surface convection. *J. Fluid Mech.* **2013**, *728*, 239–278.
- (22) Kim, S. J.; Ko, S. H.; Kang, K. H.; Han, J. Direct seawater desalination by ion concentration polarization. *Nat. Nanotechnol.* **2010**, *5*, 297–301; *Nat. Nanotechnol.* **2013**, *8*, 609.
- (23) Nam, S.; Cho, I.; Heo, J.; Lim, G.; Bazant, M. Z.; Moon, D. J.; Sung, G. Y.; Kim, S. J. Experimental Verification of Overlimiting Current by Surface Conduction and Electro-osmotic Flow in Microchannels. *Phys. Rev. Lett.* **2015**, *114*, 114501.
- (24) Zaltzman, B.; Rubinstein, I. Electro-osmotic slip and electroconvective instability. *J. Fluid Mech.* **2007**, *579*, 173–226.
- (25) Rubinstein, S. M.; Manukyan, G.; Staicu, A.; Rubinstein, I.; Zaltzman, B.; Lammertink, R. G. H.; Mugele, F.; Wessling, M. Direct observation of a nonequilibrium electro-osmotic instability. *Phys. Rev. Lett.* **2008**, *101*, 236101.
- (26) Kwak, R.; Pham, V. S.; Lim, K. M.; Han, J. Shear Flow of an Electrically Charged Fluid by Ion Concentration Polarization: Scaling Laws for Electroconvective Vortices. *Phys. Rev. Lett.* **2013**, *110*, 114501.
- (27) Rubinstein, I.; Zaltzman, B. Equilibrium Electroconvective Instability. *Phys. Rev. Lett.* **2015**, *114*, 114502.
- (28) Andersen, M. B.; van Soestbergen, M.; Mani, A.; Bruus, H.; Biesheuvel, P. M.; Bazant, M. Z. Current-induced membrane discharge. *Phys. Rev. Lett.* **2012**, *109*, 108301.
- (29) Yaroshchuk, A.; Zholkovskiy, E.; Pogodin, S.; Baulin, V. Coupled Concentration Polarization and Electroosmotic Circulation near Micro/Nanointerfaces: Taylor-Aris Model of Hydrodynamic Dispersion and Limits of Its Applicability. *Langmuir* **2011**, *27*, 11710–11721.
- (30) Licon Bernal, E.; Kovalchuk, V.; Zholkovskiy, E.; Yaroshchuk, A. Hydrodynamic dispersion in long microchannels under conditions of electroosmotic circulation. I. Non-electrolytes. *Microfluid. Nanofluid.* **2015**, *18*, 1139–1154.
- (31) Nielsen, C. P.; Bruus, H. Concentration polarization, surface currents, and bulk advection in a microchannel. *Phys. Rev. E* **2014**, *90*, 043020.
- (32) Han, J.-H.; Khoo, E.; Bai, P.; Bazant, M. Z. Over-limiting current and control of dendritic growth by surface conduction in nanopores. *Sci. Rep.* **2014**, *4*, 7056.
- (33) Suss, M. E.; Mani, A.; Zangle, T. A.; Santiago, J. G. Electroosmotic pump performance is affected by concentration

polarizations of both electrodes and pump. *Sens. Actuators, A* **2011**, *165*, 310–315.

(34) Wang, Y.-C.; Stevens, A. L.; Han, J. Million-fold Preconcentration of Proteins and Peptides by Nanofluidic Filter. *Anal. Chem.* **2005**, *77*, 4293–4299.

(35) Moya, A. A.; Belashova, E.; Sístat, P. Numerical simulation of linear sweep and large amplitude ac voltammetries of ion-exchange membrane systems. *J. Membr. Sci.* **2015**, *474*, 215–223.

(36) Zangle, T. A.; Mani, A.; Santiago, J. G. Effects of Constant Voltage on Time Evolution of Propagating Concentration Polarization. *Anal. Chem.* **2010**, *82*, 3114–3117.

(37) Yao, S.; Hertzog, D. E.; Zeng, S.; Mikkelsen, J. C.; Santiago, J. G. Porous glass electroosmotic pumps: design and experiments. *J. Colloid Interface Sci.* **2003**, *268*, 143–153.

(38) Yao, S.; Santiago, J. G. Porous glass electroosmotic pumps: theory. *J. Colloid Interface Sci.* **2003**, *268*, 133–142.

(39) Vanysek, P. Equivalent Conductivity of Electrolytes in Aqueous Solution. In *CRC Handbook of Chemistry and Physics*, 96th ed.; Haynes, W. M., Ed.; CRC Press: Boca Raton, FL, 2015–2016; pp 5–75.

(40) Yip, N. Y.; Elimelech, M. Thermodynamic and Energy Efficiency Analysis of Power Generation from Natural Salinity Gradients by Pressure Retarded Osmosis. *Environ. Sci. Technol.* **2012**, *46*, 5230–5239.

(41) Harkare, W.; Adhikary, S.; Narayanan, P.; Bhayani, V.; Dave, N.; Govindan, K. Desalination of brackish water by electrodialysis. *Desalination* **1982**, *42*, 97–105.